Waste Management 209 (2026) 115175

Contents lists available at ScienceDirect

Waste Management

journal homepage: www.elsevier.com/locate/wasman

Research paper

Black plastic identification by hyperspectral imaging in mid-wave infrared

Lukas Roming *, Felix Kronenwett, Paul Bäcker, Jerardh Josekutty, Georg Maier, Thomas Längle

Fraunhofer IOSB, Institute of Optronics, System Technologies and Image Exploitation, Fraunhoferstraße 1, Karlsruhe, 76131, Baden-Württemberg, Germany

ARTICLE INFO

Keywords:
Black plastics
Plastic recycling
Polymer identification
Hyperspectral imaging
Mid-wave infrared
Near-infrared
Convolutional neural networks
Machine learning
Waste sorting

ABSTRACT

Sensor-based sorters operating in the Near-Infrared (NIR) range are commonly used to sort post-consumer plastics. However, this method fails, when the NIR light is fully absorbed by carbon black pigments, which are present in black plastics. Mid-Wave Infrared (MWIR) is less absorbed by carbon black and therefore provides a promising alternative wavelength range for analyzing black polymers. This study compares MWIR to NIR hyperspectral imaging for classifying black and colored plastic waste. We collected spectral data from five common polymers found in post-consumer packaging, namely High-Density Polyethylene (HDPE), Low-Density Polyethylene (LDPE), Polyethylene Terephthalate (PET), Polypropylene (PP), and Polystyrene (PS). We classified the spectra using several chemometric methods, including a convolutional neural network (CNN). The results quantitatively verify the superior performance of MWIR over NIR for classifying black plastics. MWIR achieved a balanced accuracy of 83.4 % compared to 47.5 % for NIR, when using a CNN, which outperformed other chemometric methods for all sensors and sample sets. On the other hand, NIR surpasses MWIR by 7 percentage points for colored plastics in balanced accuracy. These findings suggest that MWIR hyperspectral imaging is an effective alternative to NIR hyperspectral imaging for sorting post-consumer packaging waste, especially when the share of black plastics is high.

1. Introduction

Waste management remains one of the most pressing environmental challenges of the 21st century, with global plastic waste generation reaching unprecedented levels. Recent projections indicate that global plastic use will increase from 464 Mio. t in 2020 to between 735 and 884 Mio. t by 2050, with plastic waste quantities expected to double during this period despite anticipated improvements in recycling rates (Dokl et al., 2024). The environmental consequences of plastic waste mismanagement have become increasingly evident, from microplastic pollution in oceans and freshwater systems to greenhouse gas emissions from incineration (Andrady, 2015).

In response to these challenges, numerous jurisdictions have implemented ambitious recycling targets and regulatory frameworks. The European Union, through Directive (EU) 2018/852 as part of its broader circular economy strategy, has established a 55% recycling target for plastic packaging by 2030 (Parliament and Council, 2018). This commitment was later reinforced by the European Commission's 2020 Circular Economy Action Plan, which further strengthened the EU's approach to sustainable packaging and waste management (European Commission, 2020). Separately, the UK Plastics Pact, a collaborative initiative led by WRAP (Waste and Resources Action Programme), aims for 70% of plastic packaging to be effectively recycled or composted by 2025 (WRAP, 2025). These initiatives highlight the critical importance of efficient recycling of plastic packaging waste.

To enable effective recycling, the material must be sorted by polymer type before chemical recycling. Near-Infrared (NIR) spectroscopy has become the industrial standard for automated plastic sorting in waste disposal facilities, thanks to its cost-effectiveness and rapid analysis capabilities. However, it faces a significant limitation when applied to black plastics (Rozenstein et al., 2017).

The carbon black pigments used in black plastics absorb radiation across the visible and NIR spectrum (750–2500 nm), effectively rendering these materials "invisible" to conventional NIR-based sorting systems (Becker et al., 2017). This technical limitation in sorting black plastics via NIR has substantial practical consequences, as these materials are prevalent in waste streams like electronics, automotive components, and lightweight packaging significantly hindering recycling efforts. Without effective sorting technologies, these materials are typically diverted to landfills or incineration, representing both a loss of valuable resources and a failure to meet increasingly stringent recycling targets (Rozenstein et al., 2017). This technological barrier

* Corresponding author.
E-mail address: lukas.roming@iosb.fraunhofer.de (L. Roming).

https://doi.org/10.1016/j.wasman.2025.115175
Received 7 July 2025; Received in revised form 5 September 2025; Accepted 29 September 2025
Available online 8 October 2025

has prompted exploration of alternative identification methods operating in different wavelength ranges, with Mid-Wave Infrared (MWIR) spectroscopy emerging as a particularly promising approach (Becker et al., 2017).

Hyperspectral imaging combines spectroscopy with imaging technology, collecting spectral information across hundreds of contiguous wavelength bands for each pixel in an image. In the context of plastic recycling, this enables the simultaneous identification of material composition and spatial distribution. Recent technological developments have made MWIR hyperspectral cameras commercially available, such as the Specim FX50, which operates in the 2.7–5.3 μm wavelength range. This spectral region contains distinctive absorption features for various polymers that remain detectable even in the presence of carbon black pigments that obstruct NIR analysis (Specim, Spectral Imaging Ltd., 2025).

In this study, we conduct a comprehensive evaluation of MWIR hyperspectral imaging for black plastic identification, comparing its performance to industry-standard NIR technology. Our investigation employs multiple classification approaches, including common chemometric methods (linear discriminant analysis and partial least squares discriminant analysis) and modern machine learning techniques (multilayer perceptron and convolutional neural network). We analyze both black and colored plastic samples from five common polymer types found in lightweight packaging waste: High-Density Polyethylene (HDPE), Low-Density Polyethylene (LDPE), Polyethylene Terephthalate (PET), Polypropylene (PP), and Polystyrene (PS). The results of this study offer valuable insights for the recycling industry considering investment in MWIR hyperspectral technology for black plastic sorting.

2. Related works

MWIR spectroscopy, operating in the spectral range of approximately 3–12 μm, has emerged as a leading alternative for black plastic identification. This technique probes fundamental molecular vibrations that remain detectable even in the presence of carbon black (Rozenstein et al., 2017; Signoret et al., 2019). Pioneering research, such as the work by Becker et al. (2017), and the development of MWIR-based approaches for post-consumer black plastic sorting (Rozenstein et al., 2017), have demonstrated its efficacy. Although these studies show promising results, most of them utilized a single detector without spatial resolution, like the FTIR spectroscopy, which is not suitable for an integration into a sorting system. Instead, an appropriate spatial resolution is needed (usually several hundreds of pixels). This can be achieved by whiskbroom imaging for single detectors, pushbroom imaging for line-scanning hyperspectral camera, or area imaging (Elmasry et al., 2012). Whiskbroom imaging can be time-consuming, making it challenging to integrate into a real-time sorting process. In contrast, hyperspectral cameras utilizing pushbroom imaging provide an efficient balance between scanning speed and spectral resolution.

Suppliers of MWIR hyperspectral cameras, including the Specim FX50 (2.7–5.3 μm) employed in this study, claim to offer practical solutions for identifying black polymers like Polyethylene (PE), Polypropylene (PP), Polystyrene (PS), and Polyethylene Terephthalate (PET) in sorting facilities (Specim, Spectral Imaging Ltd., 2025). One of the few literature sources on sorting experiments using MWIR technology is provided by Kruhme (2018). His research illustrates the efficiency and practical applicability of sorting black plastics within a realistic sorting scenario, employing two MWIR systems alongside a laser-induced fluorescence spectroscopy-based sorter.

Beyond MWIR, other technologies have been explored for black plastic characterization. Raman spectroscopy, which analyzes inelastic light scattering, can identify black polymers as its signal is not typically obscured by carbon black (Bae et al., 2016; Roh et al., 2017). Other approaches include Long-Wave Infrared (LWIR) spectroscopy (Larsen et al., 2024), fluorescence spectroscopy (Gruber et al., 2019), terahertz time-domain spectroscopy (Cielecki et al., 2023), and terahertz imaging (Küter et al., 2018).

Multisensor systems have been investigated for the identification of black plastics as well, leveraging the complementary strengths of different modalities. de Lima Ribeiro et al. (2024) proposed a sequential approach that combines hyperspectral reflectance imaging with Raman point sensors, with machine-learning–based data fusion to improve classification.

Another approach is to incorporate polymer-specific markers that are easily detected without affecting appearance or recyclability. Marker candidates include organic fluorophores, inorganic phosphors, and upconversion materials (Larder and Hatton, 2022; Olscher et al., 2022). Olscher et al. (2022) identified PTCDA, CeO_2, and Y_2O_3 as promising tracers, which can be used for high-value polymers such as POM.

Regardless of the approach, most of the sensors used for polymer identification output high-dimensional spectral data, which necessitates advanced analytical methods. Machine learning (ML) is crucial for classifying polymers from complex spectral data (Coleman, 2025). Techniques range from traditional chemometric methods like Linear Discriminant Analysis (LDA) and Partial Least Squares Discriminant Analysis (PLS-DA) to more advanced algorithms such as Artificial Neural Networks (ANNs) and Convolutional Neural Networks (CNNs) (Tamin et al., 2023). These algorithms enable automated and robust identification by learning the distinct spectral patterns of different polymers.

This study builds on the aforementioned advancements by evaluating MWIR hyperspectral imaging coupled with various ML classifiers for the identification of common black and colored plastic types, aiming to provide further empirical evidence for its effectiveness in enhancing post-consumer plastic recycling. By comparing results of MWIR- and NIR-based polymer identification, we provide insight into the advantages and disadvantages of both sensor technologies.

3. Materials and methods

In this section, we describe the investigated samples and spectral analysis methods employed in the study. We detail the sample collection, spectral data acquisition, and classification processes of the plastic samples.

3.1. Black plastic dataset

The black samples are uncleaned post-consumer plastics provided by the waste disposal company Lobbe RSW GmbH in Iserlohn, Germany. No pretreatment has been done to preserve the original condition of the waste samples, in which they would be sorted in the sorting plant. In total, 48 presorted samples are given as shown in Table 1. The classes are common polymer types in lightweight packaging: HDPE, LDPE, PET, PP, and PS. A few of the samples can be seen in Fig. 1. The samples were provided presorted by polymere type and we did a cross-check with measurements using an FTIR spectrometer.

3.2. Colored plastic dataset

For an initial comparison of the sensor technologies of the different wavelength ranges, a dataset consisting of colored plastic waste was created. Packaging waste from household garbage was collected and cleaned aiming at a diverse and realistic sample composition. The dataset comprises 82 samples of the polymers PET, HDPE, LDPE, PP and PS as listed in Table 1. The identification of the actual polymer type of the samples (groundtruth class) was carried out using the Resin Identification Code (RIC) and a cross-check with an FTIR spectrometer. There are at least 13 samples of each plastic type, with PP as the largest proportion of 25 samples. The properties of the samples are very diverse in terms of thickness, surface properties and transparency. The classes PP and especially LDPE contain most of the films, which are usually characterized by high transparency and a thickness of 2 to 500 μm. The PET class is dominated by bottle waste and is therefore usually

Fig. 1. A few of the samples used in this study. Left: uncleaned black plastic samples from the waste disposal company Lobbe RSW GmbH in Iserlohn, Germany. Right: colored plastic samples self-collected and cleaned.

Table 1
Number of analyzed plastic samples by polymer type and color. Samples are categorized into films and non-films, with LDPE comprising the majority of film samples.

Polymer type	Black plastics			Colored plastics		
	Films	Non-films	Total	Films	Non-films	Total
HDPE	0	10	10	1	12	13
LDPE	10	0	10	15	1	16
PET	0	4	4	0	14	14
PP	0	14	14	9	16	25
PS	0	10	10	0	14	14
Total	10	38	**48**	25	57	**82**

somewhat thicker and firmer, but mostly transparent. Packaging labels are removed from the samples.

3.3. Measurement setup

In our measurement setup, we utilized a Specim FX50 hyperspectral camera equipped with a 45-degree lens, positioned at a height of 600 mm above the scanning plate. This configuration provided a scan width of 300 mm. For the linear stage, we employed the Specim LabScanner 100 × 50. Illumination was achieved using two thermal illumination units, mounted 266 mm above the linear stage to ensure optimal focus.

The scanning was conducted at a speed of 70 mm s^{-1}, with a frame rate of 100 fps and full resolution. This setup resulted in an output resolution of 640 pixels in width, 466 lines, and 308 spectral bands. The acquisition used an integration time of 1 ms.

For the NIR recordings, the Specim FX17 was used together with a 38-degree lens and the Specim Labscanner 40 × 20. The light source consists of 6 halogen lamps. As a result, the camera delivers images with a width of 640 pixels, each with 224 spectral bands in the wavelength range from 900 to 1700 nm.

3.4. Spectral dataset

In this section, we provide an overview of the process from raw hyperspectral images to the spectral dataset used in our analysis. We outline the methodologies employed, including the spectral calibration and spatial masking. Although most of the methodologies used for MWIR are the same as for NIR, some differ, like the white balancing or removal of the CO_2 absorption band. We will focus on the process for the MWIR hyperspectral images, since it is less covered by literature and refer to the sources (Serranti et al., 2011; Roming et al., 2025) regarding the processing of the NIR hyerspectral images.

3.4.1. White balancing

First, we describe the white balancing of the MWIR spectral data. Given the wide range of reflectance in our samples, we implemented a dual integration time approach. A heated aluminum plate served as the white reference. The dual integration time approach involves using a longer integration time for the samples (t_l) than for the white reference (t_s). The normalization is performed using the formula

$$\text{Normalized Data} = \frac{\text{Data}_{t_l} - \text{Dark}_{t_l}}{\text{White}_{t_s} - \text{Dark}_{t_s}} \cdot \frac{t_s}{t_l}, \tag{1}$$

ensuring accurate white balancing by compensating for the differences in integration times between the sample and the reference measurements.

An example of white balanced HDPE MWIR spectra can be seen in Fig. 2. Before white balancing, the CO_2 absorption band is clearly visible around 4260 nm and the influence of the illumination and sensor sensitivity can be seen by the decreasing intensity at both ends of the spectral curvature. After white balancing, both effects are reduced. Still, a little influence of the CO_2 absorption band can remain, which can be seen in Fig. 4. A reason for that could be a change of CO_2 concentration or temperature between acquisition of the white reference and the sample.

3.4.2. Spectral dataset from hyperspectral images

To extract relevant spectra from hyperspectral images, pixel masks have to be created to define in which part of the image the sample is located. The masks of the colored samples were drawn by hand, whereas for the black samples, the labeler were supported by machine-learning techniques to partially automate the label-process.

After defining the masks, samples are divided into train and test sets. We conducted cross-validation using 10 independent random train–test splits, which proved essential for obtaining reliable performance estimates. Variability was driven by a subset of particularly challenging samples (e.g. spectra with low signal due to self-shadowing or items with inscriptions or stickers). Consequently, performance depended on whether these difficult cases appeared in the training or test partitions. For the artificial neural networks, we further divided the training data into a part for training and the rest for validation to select the best parameter set during training phase. From each sample, a fraction of the spectra is extracted for spectral analysis. In total, each of the four datasets (black MWIR, black NIR, colored MWIR, colored NIR) consists of 9300 spectra.

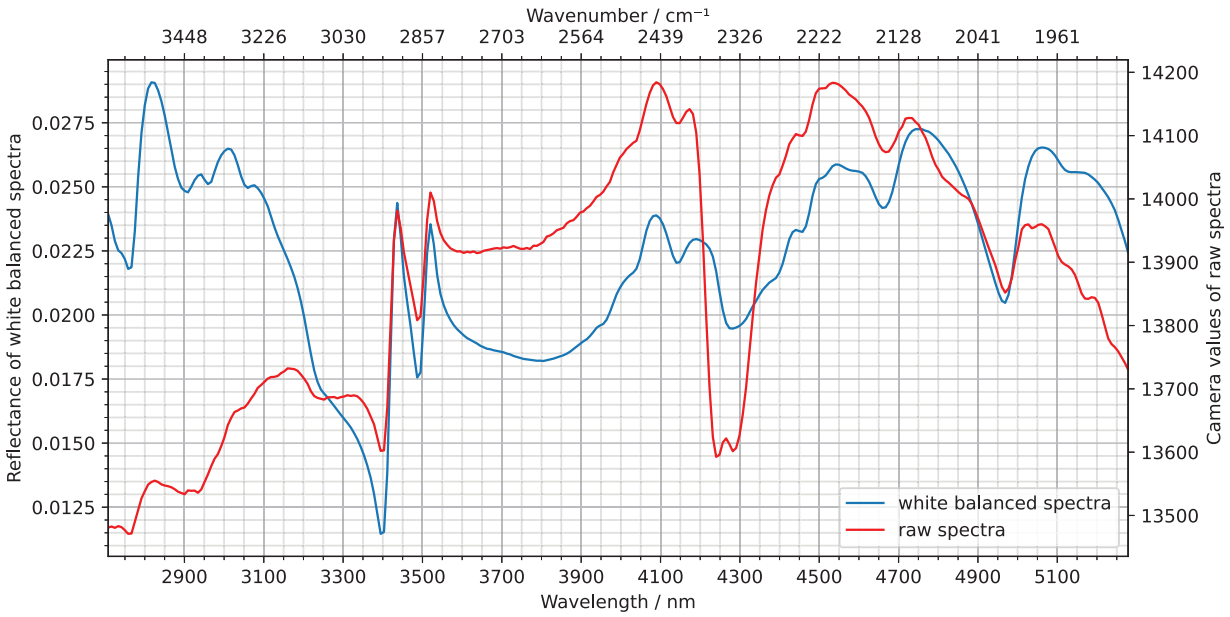

Fig. 2. MWIR spectra of HDPE before and after white balancing. In the raw spectra, the CO_2 absorption band is clearly visible around 4260 nm and the influence of the illumination and sensor sensitivity can be seen by the decreasing intensity at both ends of the spectral curvature. Both effects are reduced in the white balanced spectrum. (For interpretation of the references to color in this figure legend, the reader is referred to the web version of this article.)

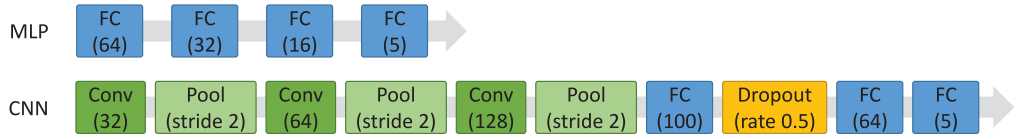

Fig. 3. Model architectures of investigated artificial neural networks. Top: MLP with fully-connected (FC) layers only. Bottom: CNN adapted from Xia et al. (2021) with convolutional, max-pooling, FC, and dropout layers. For FC and convolutional layers, the number of neurons (feature maps for convolutions) is given in brackets.

We remove the part of the spectra that is influenced by the CO_2 concentration in the air for all experiments. Therefore, all data points in the band from 4173 nm to 4383 nm are excluded. When applying statistical models to classify the materials, the spectral response in the CO_2 region can mislead the model or even lead to unwanted behaviors, like finding correlations between the polymer to predict and the CO_2 content in the air at the time the sample was measured. By predicting the CO_2 content, the model could conclude the time of measurement and thereby the underlying sample, since all samples were measured one after the other.

3.5. Applied algorithms

To classify the spectral data, five different classifiers have been investigated. The first three are common chemometric methods: PLS-DA, LDA, and spectral angle mapper (SAM). Moreover, we include artificial neural networks in our analysis, inspired by the recent advancements of these methods in near-infrared spectroscopy (Xia et al., 2021; Roming et al., 2025).

For LDA and PLS-DA we used standard normal variate (SNV) and Savitzky–Golay filtering with first derivative as preprocessing steps of the spectral data. For SAM, we applied Savitzky–Golay filtering with second derivative and excluded SNV, as it does not influence the spectral angle. For each experiment, we selected the ordering of SNV and Savitzky–Golay filtering that produced the highest evaluation scores.

We implemented a multilayer perceptron (MLP), which consists purely of fully-connected layer as depicted in Fig. 3. The input size is 283, which is the number of data points in a spectrum after removing the CO_2 band. The output size of 5 is equal to the number of classes to predict.

A convolutional neural network (CNN) using convolution along the spectral dimension is also implemented. We followed the architecture proposed by Xia et al. (2021), which gives the best results compared to other implemented CNNs. A pooling layer with stride two is added after each 1-dimensional convolutional layer. The head of the model consists of fully-connected layers and a dropout layer with a dropout rate of 0.5 as shown in Fig. 3.

4. Results

The results of this study are organized into four sections. First, the spectral analysis of attributes within the MWIR range is presented. Next, we evaluate the classification of black plastic samples using MWIR and NIR hyperspectral imaging, before evaluating colored samples. Finally, we present confusion matrices for the best-performing model to compare performance across sensors and materials and to analyze sources of misclassifications.

4.1. Spectral attributes of the plastic samples

When analyzing MWIR spectra, several polymer-specific features, especially absorption bands, can be observed. These features are related to the chemical bonds of molecules, which are excited by infrared light. This causes functional group vibrations, bond stretching and bending modes within the material and thereby absorbs energy in specific wavelength bands.

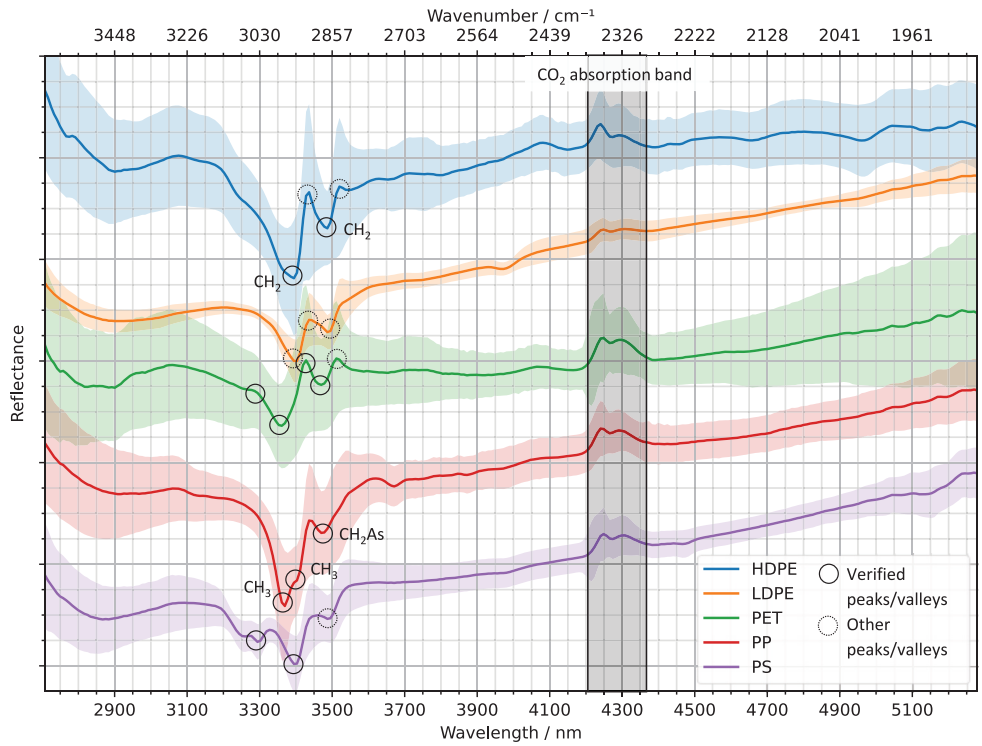

Fig. 4. Polymer reflectance spectra in the MWIR wavelength range. The values are normalized mean spectra with standard deviation for all black samples. Additionally, different offsets are added to each curve for visualization purposes. Relevant features being peaks/valleys are marked with circles. The CO_2 absorption band highlighted in gray is compensated through white balancing. (For interpretation of the references to color in this figure legend, the reader is referred to the web version of this article.)

In reflectance spectra, absorption bands are visible as low points, which can be seen in Fig. 4. The figure shows the mean spectra of the polymers with their standard deviation as a confidence band around the mean. Different vertical offsets are added to the spectra for visualization purposes. The circles in Fig. 4 highlight features of the spectra within the C-H stretching region from 3250 nm to 3550 nm (3077 to 2817 cm^{-1}). These features are related to C-H asymmetric and symmetric vibrations. Features enclosed by solid-line circles are consistent with those reported in Rozenstein et al. (2017) and Becker et al. (2017), while features marked with dotted-line circles represent observations not corroborated by other sources. Each polymer has its unique set of spectral features, yet there are similarities. For example, HDPE and PET appear to have very similar features, making it difficult to distinguish between them.

Fig. 5 shows mean reflectance spectra of all samples for the NIR and MWIR hyperspectral camera. By comparing the features in the NIR range of black and colored plastics (see bottom left and right), it becomes clear that the polymer-specific features are almost completely absent in black plastics. Note that the high point at 1420 nm is not related to the material, but the camera's spectral sensitivity and imperfections of white balancing. These effects are amplified when applying SNV to the signal of low intensity. Only for black HDPE and PET, there remain some polymer-specific features, whose intensities are significantly reduced for HDPE. A reason for the remaining features could be that the corresponding samples include different additives than the other samples to achieve the black coloration, which may not fully absorb NIR light. Nevertheless, the low signal intensity makes classification barely possible as the numbers in the results section of this work have shown.

In the MWIR range, the spectral features observed between 3250 nm and 3550 nm exhibit consistency when comparing the spectra of black and colored plastics (see top left and right of Fig. 5). Outside this wavelength region, the spectral behavior of black and colored samples differs in our experiments.

4.2. Classification results of black samples

In this section, we apply the previously described models to the recorded data and evaluate their performance using two key metrics, balanced accuracy (BA) and f1-score (F1). We selected balanced accuracy as our primary metric to address the class imbalance present in three of the four datasets under consideration. It is worth noting that for datasets with balanced class distributions, balanced accuracy is equivalent to standard accuracy. The metrics are defined by

$$\mathrm{BA} = \frac{1}{n}\sum_{i=1}^{n} \mathrm{Recall}_i$$

$$\mathrm{F1} = \frac{1}{n}\sum_{i=1}^{n} 2 \cdot \frac{\mathrm{Precision}_i \cdot \mathrm{Recall}_i}{\mathrm{Precision}_i + \mathrm{Recall}_i}$$

$$\mathrm{Precision}_i = \frac{\mathrm{TP}_i}{\mathrm{TP}_i + \mathrm{FP}_i}$$

$$\mathrm{Recall}_i = \frac{\mathrm{TP}_i}{\mathrm{TP}_i + \mathrm{FN}_i}$$

with TP_i representing true positives, TN_i true negatives, FP_i false positives, and FN_i false negatives for class i.

Fig. 6 shows the balanced accuracy (BA) and f1-score (F1) across different methods and sensors for black plastics. It can be seen that the results of all methods are considerably better when using MWIR data. All scores exceed 0.6 for the MWIR data, whereas the scores for the NIR data remain below 0.5. Still, the results on NIR data are better than random guessing, since that would lead to a balanced accuracy of 0.2 in accordance to the number of classes. When comparing the models, it turns out that CNN performed the best in all cases. Compared to more common methods, the CNN outperformed LDA by more than 2 and PLS-DA by more than 13 percentage points on MWIR data.

The fact that the CNN performance dropped from MWIR to NIR by approximately 40 percentage points, which is similar to the drop for

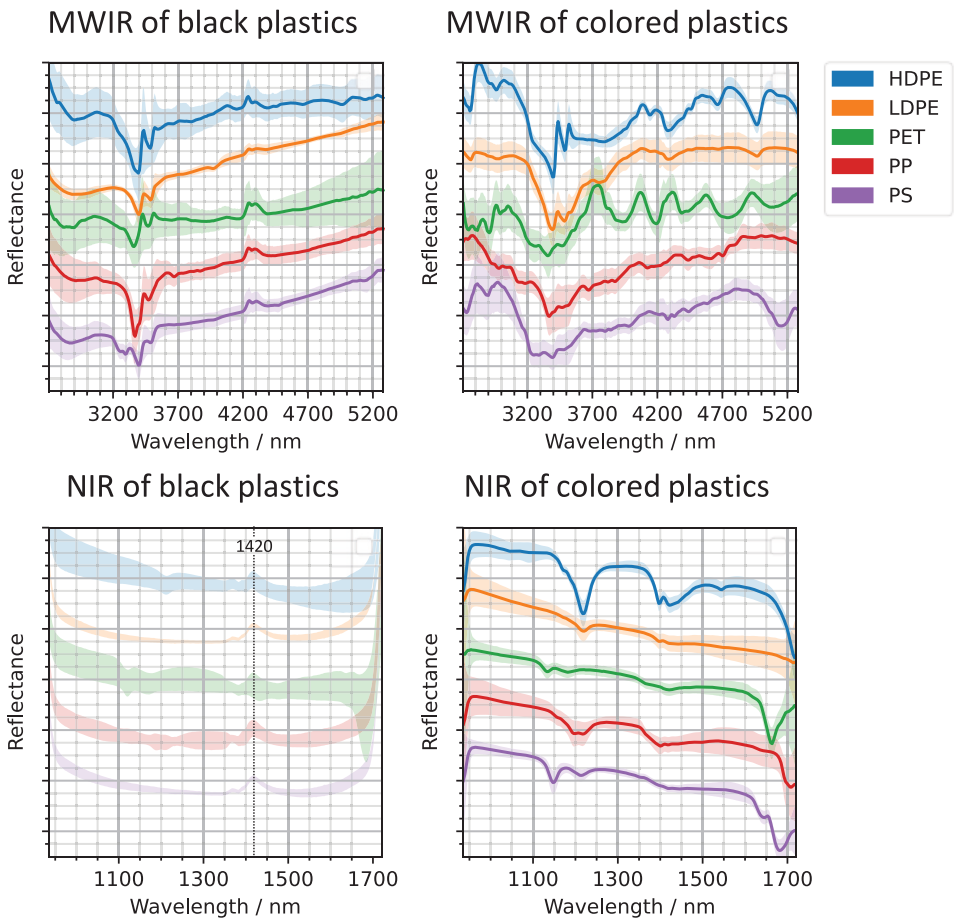

Fig. 5. Reflectance spectra in the MWIR and NIR wavelength range for black and colored plastics. The figure shows the averaged SNV-preprocessed spectra of all samples and their standard deviation. Different offsets are added to each curve for visualization purposes. (For interpretation of the references to color in this figure legend, the reader is referred to the web version of this article.)

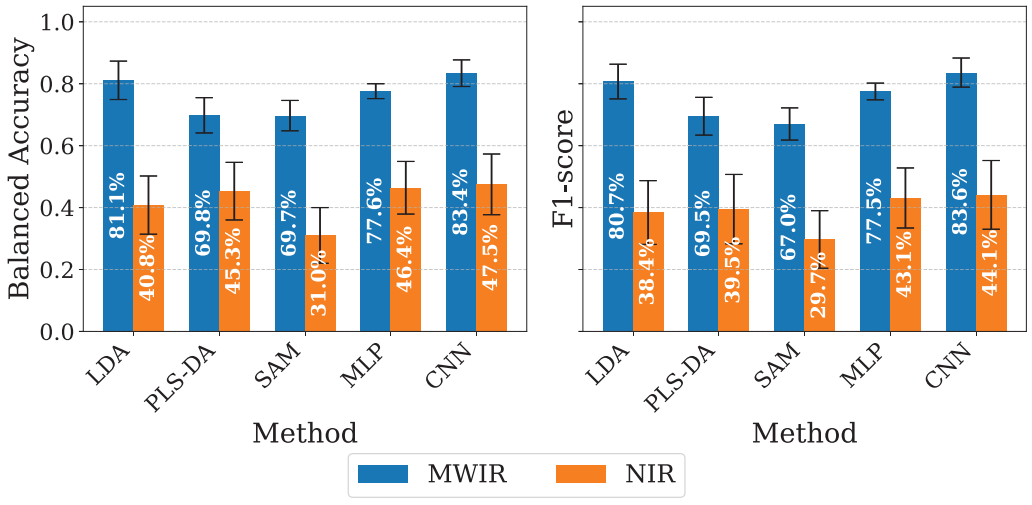

Fig. 6. Balanced accuracy and F1-score across different classification methods using NIR and MWIR sensors for black plastics. (For interpretation of the references to color in this figure legend, the reader is referred to the web version of this article.)

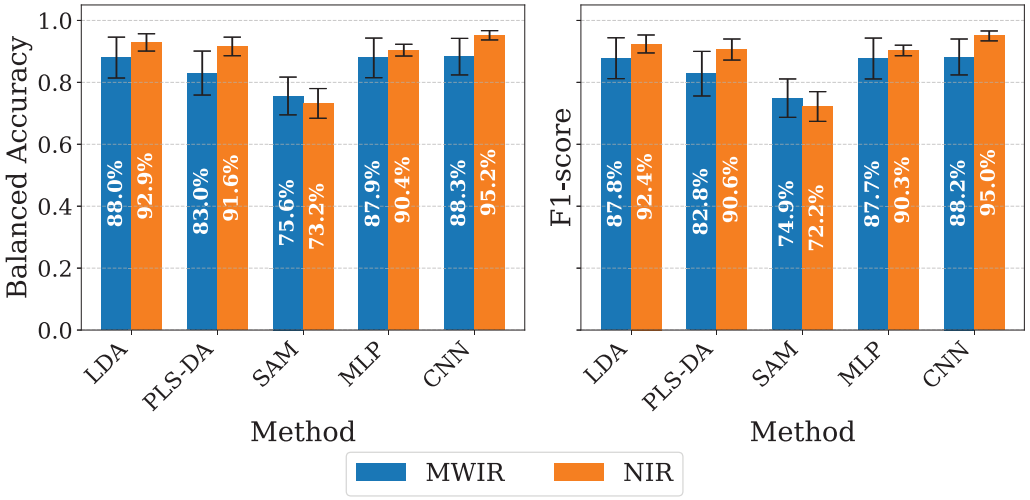

Fig. 7. Balanced accuracy and f1-score across different classification methods using NIR and MWIR sensors for colored plastics. (For interpretation of the references to color in this figure legend, the reader is referred to the web version of this article.)

LDA, demonstrates that the result is plausible. Due to the large number of trainable parameters, the CNN is prone to overfitting, and achieving unexpectedly high classification scores can be a sign of an unwanted correlation found by the model between input data and target labels. A measure that we have taken to prevent overfitting is cross-validation for 10 different random splits of the datasets. Regarding the measurement setup, we ensured a sample specific split, which means that we did not use spectra of one physical sample for train and test.

To summarize, the results show that using MWIR hyperspectral imaging, it is possible to distinguish between black plastics of the polymer types HDPE, LDPE, PET, PP, and PS. The best model (CNN) achieved a classification accuracy of 83.4%, representing a significant improvement over NIR data with 47.5%.

Note that the presented results can be improved by averaging of spectra, rejecting predictions with low confidence and improved sample pretreatment, such as removal of stickers. Since averaging the spectra or fusing the predictions within a sample depends on the sample size and the spatial resolution of the cameras, we decided to evaluate the sensors and methods by classifying each pixel separately. Moreover, the number of samples used in this study (objects, not spectra) is not high enough to estimate reliable accuracies on an object level. For example, when evaluating the CNN for MWIR on object-level by performing majority vote over the predictions within each object, all black plastic objects are correctly classified. This would make the sensor and model comparisons done before less informative, since almost all scores would be 100% and at the same time statistically less reliable.

4.3. Classification results of colored samples

We extend our investigation to the classification of colored plastics, encompassing all colors including white, but excluding black, utilizing the same sensors, methodologies, and evaluation metrics. Our goal is to determine whether MWIR spectra yield higher classification accuracy for colored materials and to assess the performance of the MWIR hyperspectral camera in comparison to a NIR hyperspectral camera. Given that NIR hyperspectral imaging is known for its efficacy with non-black polymers, we expect a closer and more competitive comparison.

Fig. 7 shows the result of this investigation. It becomes evident that the results for colored materials surpass those for black materials. For MWIR, the scores are almost 5 percentage points higher when using CNN, the best-performing model. For other models, the improvement is even higher, leading to a smaller gap to CNN. Nearly all models performed above 80% BA, whereas on black plastics, only CNN and LDA with MWIR could reach as high scores.

Although carbon black is not supposed to affect MWIR, the signal intensity of black plastics is still significantly lower compared to colored samples. This matches with the observation of Rozenstein et al. (2017) and could be the reason for the poorer classification performance on the black polymers.

Another insight that can be gained from Fig. 7 is that NIR outperforms MWIR for colored plastics in our experiments. CNN was able to classify the MWIR data with a BA of 88.3%. When using NIR data, CNN reached 95.2%, being almost 7 percentage points higher. It should be noted that the colored samples investigated are challenging, since most of them were thin foils, with some being transparent. These thin foils can be difficult for spectral analysis due to thin-film interference, which leads to an oscillating spectral signal. This occurs when the film thickness is not significantly greater than the wavelength. Thin plastic foils, typically exceeding 2 µm in thickness, have a more pronounced effect on the MWIR wavelength range compared to NIR. The spectral reflectance oscillates as a sine wave across wavenumber, potentially influencing the classifier's performance. Transparent foils, on the other hand, are problematic because the material interferes less with light, worsening the signal-to-noise ratio and thereby having a negative effect as well. As a consequence, the performance on colored materials with fewer foils can be expected to be higher than observed here, enlarging the gap between the results on colored and black plastics.

4.4. Confusion matrices of CNN

For the model with the highest BA, namely the CNN, we present the confusion matrices across both datasets and both sensors. Thereby, we aim to gain an insight into the source of the previously presented accuracy shortfalls and misclassifications, with particular (though not exclusive) attention to the MWIR sensor.

The confusion matrices in Fig. 8 show the relative frequency of predicted versus actual polymer class, enabling deeper insight into the material-specific prediction results. In the optimal case, the diagonal of the matrix would be 1 and all other values 0. The confusion matrices presented here show high values on the diagonal, except for the confusion matrix in the bottom left, which represents the results for black plastics with NIR data. Apart from black plastics, distinguishing HDPE and LDPE is also challenging for NIR, which is emphasized in the

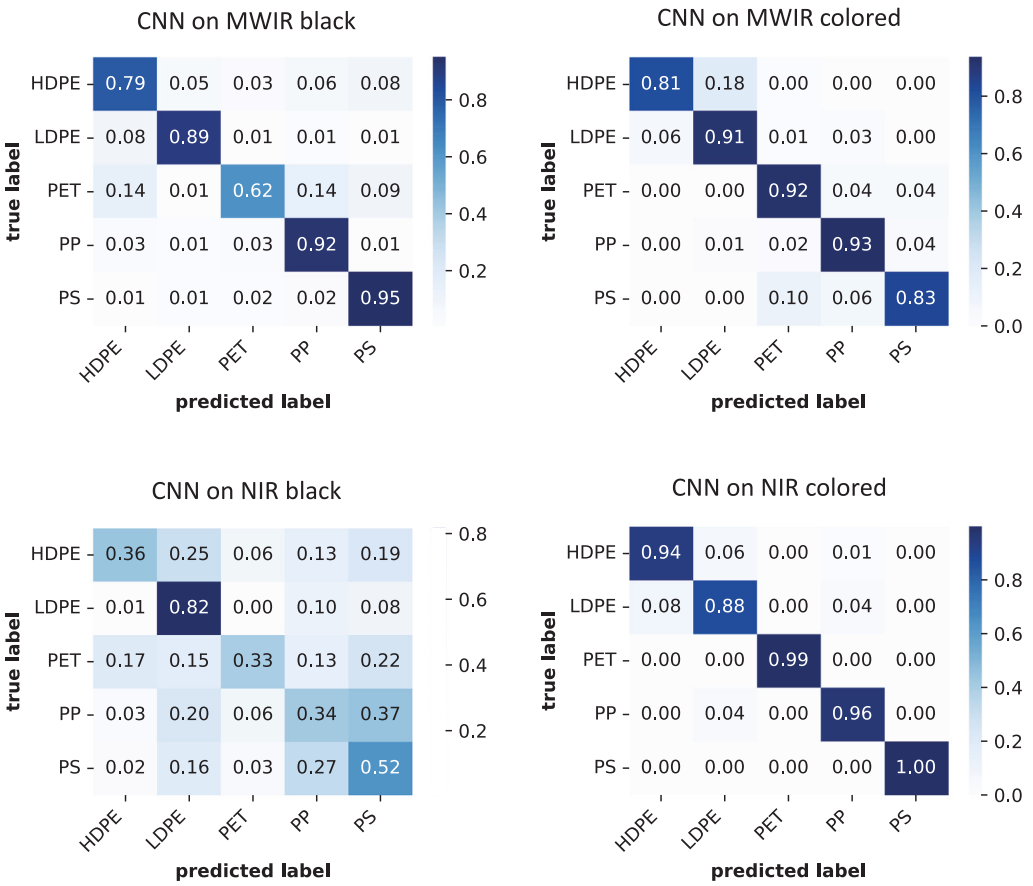

Fig. 8. Confusion matrices for the convolutional neural network (CNN), which outperformed the other models. The matrices show which polymers are correctly classified and which ones are mixed up by the classifier.

confusion matrix (bottom right), although the CNN was able to classify most of them correctly.

When looking at the MWIR confusion matrices or at the MWIR spectra 4, it seems that the similarity of HDPE and LDPE remains in MWIR. Furthermore, some new challenges arise, such as the discrimination of PET and PP, which show similarities within the MWIR spectra and exhibit slightly worse performance within the confusion matrices.

An analysis of spectra that were misclassified showed that the main reason for wrongly classified black plastic MWIR spectra is low signal intensity. This was caused by shadowing from the sample geometry, specular surfaces that appear dark in the line scan setup, or broadband absorption through the material. We observed low-signal MWIR spectra more often in our black PET samples, which reduced PET-class accuracy (top left of Fig. 8). A similar issue occurred for HDPE, whereby one specimen had dark, self-shadowed regions due to its geometry. Plastic products typically carry product labels, but their overall impact on MWIR classification was limited. Label-related errors were caused by attenuated signal or specular behavior, likely due to metallic components in the labels.

5. Conclusions

In this study, the spectral analysis and classification of black and colored plastic samples using MWIR and NIR hyperspectral imaging systems were investigated. The analysis of polymers by MWIR hyperspectral imaging reveals distinct spectral features associated with specific chemical bonds, particularly within the C-H stretching region. However, similarities between polymers, such as HDPE and PET posed classification challenges. The classification results demonstrated that MWIR data provided superior performance in identifying black plastic samples, with the CNN model achieving a balanced accuracy of 83.4% compared to 47.5% for NIR data. For colored samples, all accuracies were notably higher, with CNN achieving a balanced accuracy of 95.2% using NIR data, outperforming MWIR by approximately 7 percentage points. While MWIR hyperspectral imaging effectively differentiates black plastic types, NIR provides better discrimination for colored samples in our experiments, especially for those with challenging characteristics such as thin or transparent foils. These findings suggest that, in contrast to NIR, MWIR can be used to sort black plastics effectively, but could slightly compromise the sorting results of colored plastics. Note that enhanced results can be achieved by averaging spectra from multiple pixels within a sample.

Finally, it should be noted that MWIR technology is more cost-intensive and requires an infrared heater, increasing the need for measures to prevent overheating. Combining NIR and MWIR sensors for plastics sorting could offer the best solution in terms of sorting purity. Similarly, extending the wavelength range to the fingerprint region of up to 15 µm (650 cm^{-1}) could also improve accuracy.

CRediT authorship contribution statement

Lukas Roming: Writing – original draft, Visualization, Validation, Software, Methodology, Investigation. **Felix Kronenwett:** Writing – original draft, Validation, Software, Investigation. **Paul Bäcker:** Writing – original draft, Validation, Software, Investigation. **Jerardh Josekutty:** Writing – original draft, Visualization. **Georg Maier:** Writing – review & editing, Supervision, Funding acquisition, Conceptualization. **Thomas Längle:** Funding acquisition.

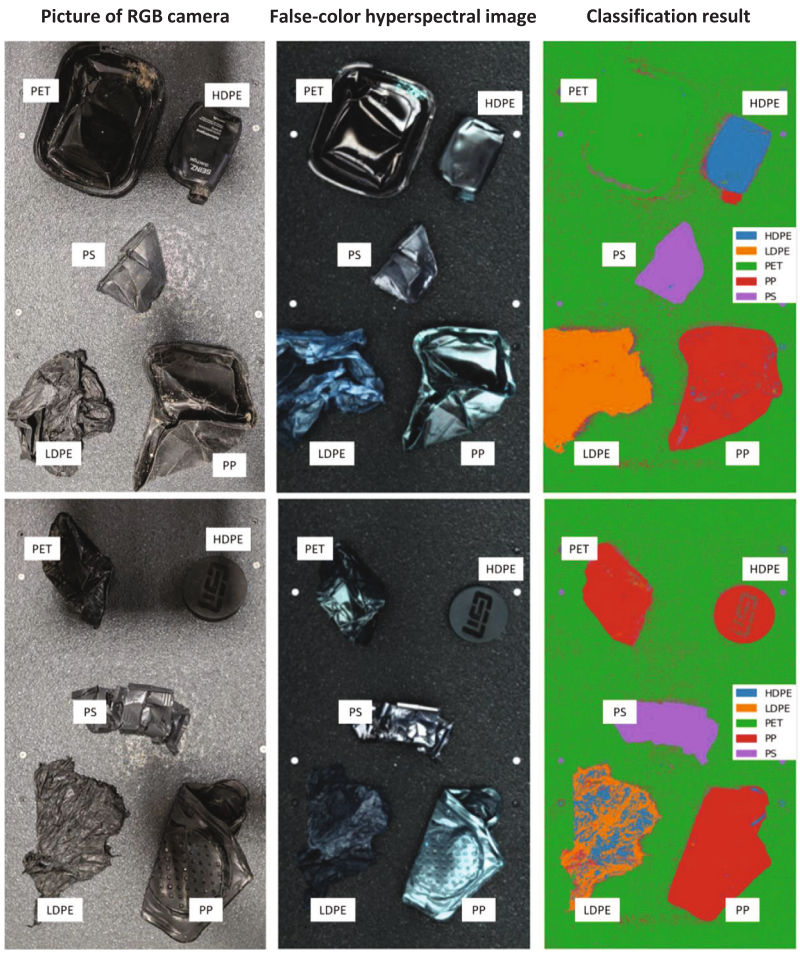

Fig. A.9. Left: Photograph of a few black plastic samples. Middle: false-color image of MWIR hyperspectral camera. Right: Prediction result of CNN given by classifying each pixel of the hyperspectral MWIR image. (For interpretation of the references to color in this figure legend, the reader is referred to the web version of this article.)

Declaration of Generative AI and AI-assisted technologies in the writing process

During the preparation of this work the authors used FhGenie (generative AI of the Fraunhofer-Gesellschaft) and ChatGPT to improve readability and language. After using this tool/service, the authors reviewed and edited the content as needed and take full responsibility for the content of the publication.

Declaration of competing interest

The authors declare the following financial interests/personal relationships which may be considered as potential competing interests: Lukas Roming reports financial support was provided by Federal Ministry of Research, Technology and Space (BMFTR). Lukas Roming reports equipment, drugs, or supplies was provided by Lobbe Umweltservice GmbH & Co KG. If there are other authors, they declare that they have no known competing financial interests or personal relationships that could have appeared to influence the work reported in this paper.

Acknowledgments

This work is part of the K3I-Cycling project and funded by the Federal Ministry of Research, Technology and Space (BMFTR), Germany under the funding reference 033KI201.

Appendix. Prediction result on full images using CNN

When working with hyperspectral cameras, visualizing the prediction result for full images can be useful to gain further insight into the prediction results. Moreover, when comparing photographs of a sample to the hyperspectral false-color image, one can find interesting relationships. The Fig. A.9 shows the results with a photograph on the left, the hyperspectral false-color image in the MWIR wavelength range in the middle and the prediction result of CNN for each pixel in the hyperspectral image on the right. In the first sample collection of Fig. A.9, the model classified nearly everything correctly. On the sample at the top right, there is a lid, which is correctly classified differently from the bottle it belongs to. In general, lids of plastic bottles are usually made of a different material than the bottle itself, which is why we removed the lids from our train and test sets to ensure a pure material stream. In the second scenario on the lower image, the CNN performed worse. The PET and HDPE samples are wrongly classified as PP.

Data availability

Data will be made available on request.

References

Andrady, A.L., 2015. Plastics and Environmental Sustainability. John Wiley & Sons.

Bae, J.-S., Oh, S.-K., Kim, H.-K., 2016. Design of automatic classification system of black plastics based on support vector machine using Raman spectroscopy. J. Korean Inst. Intell. Syst. 26 (5), 416–422.

Becker, W., Sachsenheimer, K., Klemenz, M., 2017. Detection of black plastics in the middle infrared spectrum (MIR) using photon up-conversion technique for polymer recycling purposes. Polymers 9 (9), 435.

Cielecki, P.P., Hardenberg, M., Amariei, G., Henriksen, M.L., Hinge, M., Klarskov, P., 2023. Identification of black plastics with terahertz time-domain spectroscopy and machine learning. Sci. Rep. 13 (1), 22399.

Coleman, B.R., 2025. An introduction to machine learning tools for the analysis of microplastics in complex matrices. Environ. Sci.: Process. Impacts.

Dokl, M., Copot, A., Krajnc, D., Fan, Y.V., Vujanović, A., Aviso, K.B., Tan, R.R., Kravanja, Z., Čuček, L., 2024. Global projections of plastic use, end-of-life fate and potential changes in consumption, reduction, recycling and replacement with bioplastics to 2050. Sustain. Prod. Consum. 51, 498–518. http://dx.doi.org/10.1016/j.spc.2024.09.025, URL: https://www.sciencedirect.com/science/article/pii/S2352550924002823.

Elmasry, G., Kamruzzaman, M., Sun, D.-W., Allen, P., 2012. Principles and applications of hyperspectral imaging in quality evaluation of agro-food products: a review. Crit. Rev. Food Sci. Nutr. 52 (11), 999–1023.

European Commission, 2020. A New Circular Economy Action Plan for a Cleaner and More Competitive Europe. Communication COM(2020) 98 final, European Commission, URL: https://eur-lex.europa.eu/legal-content/EN/TXT/?qid=1583933814386&uri=COM:2020:98:FIN.

Gruber, F., Grählert, W., Wollmann, P., Kaskel, S., 2019. Classification of black plastics waste using fluorescence imaging and machine learning. Recycling 4 (4), 40.

Kruhme, S., 2018. Untersuchungen zur Sortierung dunkler thermoplastischer Kunststoffe mittels Neuentwicklungen in der Sortiertechnik (Ph.D. thesis). Technische Universität Bergakademie Freiberg.

Küter, A., Reible, S., Geibig, T., Nüßler, D., Pohl, N., 2018. THz imaging for recycling of black plastics. Tm-Tech. Mess. 85 (3), 191–201.

Larder, R.R., Hatton, F.L., 2022. Enabling the polymer circular economy: innovations in photoluminescent labeling of plastic waste for enhanced sorting. ACS Polym. Au 3 (2), 182–201.

Larsen, M.N., Jørgensen, A.L., Petrunin, V., Kjelstrup-Hansen, J., Jørgensen, B., Hinge, M., 2024. Classification of black plastic types by hyperspectral imaging based on long-wave infrared emission spectroscopy. Polym. Test. 141, 108629.

de Lima Ribeiro, A., Fuchs, M.C., Lorenz, S., Röder, C., Heitmann, J., Gloaguen, R., 2024. Multi-sensor characterization for an improved identification of polymers in WEEE recycling. Waste Manage. 178, 239–256.

Olscher, C., Jandric, A., Zafiu, C., Part, F., 2022. Evaluation of marker materials and spectroscopic methods for tracer-based sorting of plastic wastes. Polymers 14 (15), 3074.

Parliament, E., Council, 2018. Directive (EU) 2018/852 of the European Parliament and of the Council of 30 May 2018 amending Directive 94/62/EC on packaging and packaging waste. Off. J. Eur. Union L 150 (2018/852), 141–154, URL: https://eur-lex.europa.eu/legal-content/EN/TXT/?uri=CELEX:32018L0852.

Roh, S.-B., Oh, S.-K., Park, E.-K., Choi, W.Z., 2017. Identification of black plastics realized with the aid of Raman spectroscopy and fuzzy radial basis function neural networks classifier. J. Mater. Cycles Waste Manag. 19, 1093–1105.

Roming, L., Maier, G., Bäcker, P., 2025. Robust model development for HSI-based characterization of post-consumer plastics. In: OCM 2025-7th International Conference on Optical Characterization of Materials, March 26th–27th, 2025, Karlsruhe, Germany: Conference Proceedings. KIT Scientific Publishing, p. 207.

Rozenstein, O., Puckrin, E., Adamowski, J., 2017. Development of a new approach based on midwave infrared spectroscopy for post-consumer black plastic waste sorting in the recycling industry. Waste Manage. 68, 38–44.

Serranti, S., Gargiulo, A., Bonifazi, G., 2011. Characterization of post-consumer polyolefin wastes by hyperspectral imaging for quality control in recycling processes. Waste Manage. 31 (11), 2217–2227.

Signoret, C., Caro-Bretelle, A.-S., Lopez-Cuesta, J.-M., Ienny, P., Perrin, D., 2019. MIR spectral characterization of plastic to enable discrimination in an industrial recycling context: I. Specific case of styrenic polymers. Waste Manage. 95, 513–525.

Specim, Spectral Imaging Ltd., 2025. Overcoming black plastic recycling challenge with MWIR hyperspectral imaging technology. Specim Blog/News (Accessed 25 April 2025).

Tamin, O., Moung, E.G., Dargham, J.A., Yahya, F., Omatu, S., 2023. A review of hyperspectral imaging-based plastic waste detection state-of-the-arts. Int. J. Electr. Comput. Eng.(IJECE) 13, 3407–3419.

WRAP, 2025. Progress against the targets. URL: https://www.wrap.ngo/taking-action/plastic-packaging/initiatives/the-uk-plastics-pact/progress-against-targets. (Accessed 24 April 2025).

Xia, J., Huang, Y., Li, Q., Xiong, Y., Min, S., 2021. Convolutional neural network with near-infrared spectroscopy for plastic discrimination. Environ. Chem. Lett. 19 (5), 3547–3555.